HHS Public Access

Author manuscript

Cancer Immunol Res. Author manuscript; available in PMC 2019 December 23.

Published in final edited form as:

Cancer Immunol Res. 2019 March ; 7(3): 466–475. doi:10.1158/2326-6066.CIR-18-0336.

Rapamycin prevents surgery-induced immune dysfunction in patients with bladder cancer

Robert S. Svatek[1,2,**], **Niannian Ji**[1,2], **Essel de Leon**[3], **Neelam Mukherjee**[1,2], **Aashish Kabra**[2], **Vincent Hurez**[1], **Marlo Nicolas**[3], **Joel E. Michalek**[7], **Martin Javors**[8], **Karen Wheeler**[1,2], **Z. Dave Sharp**[4,9,10], **Carolina B. Livi**[1], **Zhen-Ju Shu**[1,2], **David Henkes**[6], **Tyler J. Curiel**[1,5,**]

[1]Experimental Developmental Therapeutics (EDT) Program, Mays Cancer Center at UT Health MD Anderson, San Antonio, Texas

[2]Department of Urology, UT Health San Antonio, San Antonio, Texas

[3]Department of Pathology, UT Health San Antonio, San Antonio, Texas

[4]Department of Molecular Medicine, UT Health San Antonio, San Antonio, Texas

[5]Division of Hematology/Medical Oncology at the UT Health San Antonio, San Antonio, Texas

[6]Department of Pathology, CHRISTUS Santa Rosa Medical Center, San Antonio, Texas

[7]Department of Epidemiology and Biostatistics, UT Health San Antonio, San Antonio, Texas

[8]Department of Psychiatry, UT Health San Antonio, San Antonio, Texas

[9]The Cancer Therapy Research Center/Population Science and Prevention (PSP) Program, UT Health San Antonio, San Antonio, Texas

[10]Barshop Institute for Longevity and Aging Studies, UT Health San Antonio, San Antonio

Abstract

The mechanistic target of rapamycin (mTOR) integrates environmental inputs to regulate cellular growth and metabolism in tumors. However, mTOR also regulates T-cell differentiation and activation, rendering applications of mTOR inhibitors towards treating cancer complex. Preclinical data supports distinct biphasic effects of rapamycin, with higher doses directly suppressing tumor cell growth and lower doses enhancing T-cell immunity. To address the translational relevance of these findings, the effects of the mTOR complex 1 (mTORC1) inhibitor, rapamycin, on tumor and T cells were monitored in patients undergoing cystectomy for bladder cancer (BC). MB49 syngeneic murine BC models were tested to gain mechanistic insights. Surgery induced T-cell exhaustion in humans and mice and was associated with increased pulmonary metastasis and decreased PD-L1 antibody efficacy in mouse BC. At 3 mg orally daily, rapamycin concentrations

[**]**Authors for Correspondence:** Tyler J. Curiel, MD, MPH, Department of Medicine, Division of Hematology-Oncology, University of Texas Health San Antonio, the Mays Family Cancer Center, 7703 Floyd Curl Dr., San Antonio, TX 78229, Office: 210-567-6691, curielt@uthscsa.edu; Robert S. Svatek, MD, MSCI, Department of Urology, University of Texas Health San Antonio, the Mays Family Cancer Center, 7703 Floyd Curl Dr., San Antonio, TX 78229, Office: 210-567-5676, svatek@uthscsa.edu.

The authors declare no potential conflicts of interest.

Trial Registration: ClinicalTrials.gov

were 2-fold higher in bladder tissues than in blood. Rapamycin significantly inhibited tumor mTORC1, shown by decreased rpS6 phosphorylation in treated versus control patients (P=0.008). Rapamycin reduced surgery-induced T-cell exhaustion in patients, evidenced by a significant decrease in the prevalence of dysfunctional programmed death-1 (PD-1)–expressing T cells. Grade 3-4 adverse event rates were similar between groups, but rapamycin-treated patients had a higher rate of wound complications versus controls. In conclusion, surgery promoted BC metastasis and decreased the efficacy of post-operative BC immunotherapy. Low dose (3 mg daily) oral rapamycin has favorable pharmacodynamic and immune modulating activity in surgical patients and has potential to decrease surgery-induced immune dysfunction.

Keywords

bladder neoplasm; mTOR; rapamycin; surgery; immune system

Introduction

Activating genetic alterations in PI3K/AKT/mTOR signaling are present in more than 40% of bladder tumors (1–6), providing justification for using mTOR inhibition to treat bladder cancer (BC) if mTOR inhibition is the sole aim. The prototypical mTOR complex 1 (mTORC1) inhibitor, rapamycin, and rapamycin analogues demonstrate effective antitumor activity in preclinical BC models (7–14) and human trials have been conducted. These trials sought the maximal tolerated dose based on the notion that higher dosing leads to improved inhibition of target tumor cell mTORC1 signaling in the BC itself. However, at standard clinical doses (*i.e.* ≥5 mg daily), these agents demonstrate only modest activity against metastatic disease (15–17) and are too toxic for treatment of less advanced disease (11,16,17).

In addition to driving tumor growth, mTOR signaling also regulates activation and differentiation of many cell types, including T cells, which mediate antitumor immunity (18–21). We previously showed distinct effects of rapamycin in cancers across dose and tissue types with higher doses (1-8 mg/kg/day) directly suppressing tumor cell growth, whereas lower doses (0.075 mg/kg/day) enhanced T-cell immunity (18). Potential beneficial immune effects of lower dose mTORC1 inhibition is also supported by data from non-cancer patients, showing that at 0.5 mg daily or 5-20 mg weekly, everolimus, a rapamycin analogue, improves antibody immune responses to an influenza vaccine and reduces the prevalence of programmed death -1 (PD-1)–positive T cells (22). PD-1 is a marker of T-cell exhaustion, a common feature of chronic infections (23) and cancer (24) characterized by ineffective pathogen control or tumor eradication.

To determine the pharmacodynamic and T-cell effects of oral rapamycin in patients with BC undergoing cystectomy, we conducted a pre-surgical clinical trial. This approach enabled evaluation of paired patient tissues serially collected during treatment to examine drug delivery and target tissue specificity (25). Comparison of immune cells collected before and after cystectomy revealed a significant increase in T cells expressing PD-1 following cystectomy, suggesting that surgery could inhibit antitumor immunity. We studied clinical

potential using the syngeneic MB49 mouse bladder tumor model. Surgery increased lung metastasis and reduced response to PD-L1 antibody immunotherapy in this model. These findings characterize untoward effects of surgery on T-cell function and response to cancer immune therapy and could influence perioperative treatment strategies.

Methods

Design and participants

A two-arm, open-label randomized study of rapamycin for patients (n=20) suffering from invasive urothelial BC was conducted (trial schema in Supplementary Fig. S1). The local institutional regulatory board (IRB) approved the study (IRB 12-135H), which was publicly registered (ClinicalTrials.gov identifier:). All participating patients provided written informed consent. This study's involvement with human subjects complies with the Declaration of Helsinki. Tissues collected included blood and bladder tumors and were processed for flow cytometry or immunohistochemistry (IHC) as described below. Eligible patients had invasive (clinical stage ≥T1) BC, with no evidence of nodal or visceral metastasis, Zubrod performance status of 0-2, and were unable or unwilling to receive cisplatin-based neoadjuvant chemotherapy. Additional eligibility criteria included adequate bone marrow function (defined as granulocytes >1,500 cells/mm^3, hemoglobin ≥9.5 gm/dL, and platelets >70,000/mm^3), life expectancy ≥1 year, ability to provide sufficient tumor at surgery for research purposes, and age ≥18 years. Exclusions included hepatic impairment, HIV or other chronic infections, allergy to rapamycin, or chronic steroid use. Patients with controlled medical conditions (*e.g.,* hypertension, diabetes) were eligible if they were under physician care. Enrollment occurred from May 2012 to September 2013. Cystectomy was indicated for all patients with muscle-invasive (stage ≥T2) BC and for patients with non-muscle invasive (stage T1) BC due to inability to clear disease with repeated resections.

Treatment

Patients were randomized 1:1 to received 3 mg daily oral rapamycin (Rapamune, Wyeth Pharmaceuticals, 1 mg tablets) irrespective of weight or age, or no treatment for 28 days prior to cystectomy. No dose adjustments were made, but blood concentrations were measured to monitor adherence and to correlate with tissue concentrations. The final dose was given in the morning, one day before surgery. Patients were instructed to take rapamycin 1 hour before or 2 hours after food and to avoid grapefruit juice, which inhibits cytochrome P450 CYP3A4 leading to decreased drug metabolism. Cystectomy included bladder and prostate (males) removal, bilateral pelvic lymph node dissection, and urinary diversion. Wound closure was performed with absorbable sutures (not staples) and drains were left in place until drain flow was acceptably low (≤100 cc per day) as recommended for patients on rapamycin treatment (26).

Safety

Toxicity was evaluated using the National Cancer Institute Common Toxicity Criteria version 4.02. Safety and adverse events were assessed at each clinic visit, on the day of cystectomy, every day following cystectomy while the patient was in the hospital and at follow-up visits up until 90 days after surgery. Assessments included documented medical

history, physical examination, and laboratory evaluation as appropriate. Dose-limiting toxicity was defined as grade 3 or 4 neutropenia with fever or lasting >7 days, platelets <70,000/mm^3, grade ≥3 non-hematologic toxicity, or irreversible grade 2 toxicity related to rapamycin.

Pharmacokinetics

Whole blood for rapamycin concentration measurement was collected by peripheral venipuncture into K2-ethylenediaminetetraacetic acid (EDTA) vials (BD, #367844) at 30 days after registration. At radical cystectomy, a small tissue section (approximately 5 mm^3) was taken and immediately frozen for rapamycin concentration assessments. Blood rapamycin was quantified according to previously published procedures (27–29) using tandem mass spectrometer for detection. Rapamycin concentration was not performed in one patient who discontinue rapamycin early and who refused rapamycin blood assessment. Rapamycin and ascomycin (ASCO; internal standard) were obtained from LC Laboratories (Woburn, MA). High-performance liquid chromatography (HPLC) grade methanol and acetonitrile were purchased from Fisher (Fair Lawn, NJ). All other reagents were purchased from Sigma Chemical Company (St. Louis, MO).

For human bladder tumor tissue, 100 mg of calibrator and unknown tissue samples were mixed by sonication (three 5-second bursts) with 10 μL ASCO (0.5 μg/mL, internal standard) and 300 μl of a solution containing 0.1% formic acid and 10 mM ammonium formate dissolved in 95% HPLC grade methanol. After sonication, the samples were vortexed vigorously for 2 min, and then centrifuged at 13,000 x *g* for 5 minutes at 23°C (subsequent centrifugations were performed under the same conditions). Supernatants were transferred to 1.5 mL microfilterfuge tubes, and then 40 μL of the final extracts were injected into the liquid chromatography with tandem mass spectrometry (LC-MS/MS). The ratio of the peak area of rapamycin to that of the internal standard ASCO (response ratio) for each unknown sample was compared against a linear regression of calibrator response ratios at 0, 2, 10, 20, 50, and 100 ng/g to quantify rapamycin. The concentration of rapamycin was expressed as ng/g of tissue.

Immunohistochemistry and pathologic assessments

We used phosphorylation of ribosomal protein S6 (rpS6) at serine 240/244 (assessed by immunohistochemistry, IHC) as an indirect measure of S6 kinase 1 and mTORC1 activity. An H-score was used as a semiquantitative measure of phosphorylation, determined by the percentage of cells scoring positive (0-100) multiplied by staining intensity (0-3) (30). Genitourinary pathologists blinded to treatment groups and sample pairing performed all IHC interpretations. Tissue slides were cut at 5 microns from the entire tumor within formalin-fixed, paraffin-embedded tissue blocks and subsequently probed using antibodies (Cell Signaling Technologies) for phosphorylated (Ser240/244) rpS6 (#2215), rpS6 (#2217), phosphorylated (Ser473) AKT (#4060), AKT (#4691), phosphorylated (Thr37/46) 4E-BP1 (#2855), 4E-BP1 (#9644), and PTEN (phosphatase and tensin homologue deleted on chromosome ten, #9559).

Flow cytometry

Whole blood was collected by peripheral venipuncture into lithium heparin vials (BD, #367880) at baseline and at 30 and 60 days after registration. We isolated peripheral blood mononuclear cells (PBMCs) from patient blood samples using Ficoll-Paque gradients (GE Healthcare). PBMCs were suspended in freezing medium (complete Roswell Park Memorial Institute (RPMI)) with 50% fetal bovine serum and 10% dimethyl sulfoxide (DMSO) (Corning, Fisher Scientific) and cryopreserved at −150 °C until analyzed. When sufficient tumor was available at biopsy or cystectomy, a small tumor section (approximately 5 mm^3) was excised under sterile conditions and placed into RPMI media containing 1% antibiotic and transported on ice. Tumor tissues were washed with PBS, cut into 1-2 mm pieces, and digested in 5 mL of digestion solution containing 0.05% trypsin, collagenase (1mg/mL), and DNase (0.25 mg/mL) for 45 minutes at 37°C and processed into single-cell suspensions. PBMCs were thawed in complete RPMI and counted with a Vi-cell XR (Beckman Coulter) before resuspension in flow buffer (2% fetal bovine serum in PBS).

$1x10^6$ PBMCs per sample were stained and analyzed using an LSR II flow cytometer and FACSDiva software (BD Bioscience, v6). Validated commercial reagents were used: LIVE/DEAD Fixable Aqua Dead Cell Stain Kit (Life Technologies), fluorochrome-conjugated, monoclonal anti-human CD45 (clone HI30), CD3 (clone HIT3a), CD4 (clone OKT4), CD8 (clone SK1), IFNγ (clone 4S.B3), TNFα (clone MAb11), CD62L (clone DREG-56), CD45RO (clone UCHL1), FoxP3 (clone 206D), PD-1 (clone EH12.2H7), TIM-3 (clone F38-2E2), LAG-3 (clone 3DS223H eBioscience, Invitrogen) (BioLegend). For cytokine staining, cells were stimulated with Leukocyte Activation Cocktail with GolgiPlug (BD Biosciences #550583) for 5 hours according to manufacturer's protocol. Then they were surface stained, fixed, permeabilized with fixation and permeabilization solution (BD Biosciences, #554722) according to manufacturer's protocol and then stained for intracellular cytokines.

T-cell proliferation

PBMCs were first labeled with carboxyfluorescein succinimidyl ester (CFSE) and sorted to high purity (>97%) as $CD3^+PD\text{-}1^+$ versus $CD3^+PD\text{-}1^-$ T cells using fluorescence-activated cell sorting on a FACS Aria II (BD). Then, 0.5 – 1.0 x 10^6 cells were stimulated *in vitro* with Dynabeads Human T-Activator CD3/CD28 at a bead to cell ratio of 1:1 (Life technologies) in 96-well flat-bottom plates. After 3 days, cells were stained and analyzed using flow cytometry to measure CFSE fluorescence signal of both $CD4^+$ and $CD8^+$ T cells in sorted populations (Supplementary Fig. S2). CFSE in medium control samples of each T-cell subset was used as the baseline for gating proliferated populations. Samples from all patients and time points were run simultaneously using v6 FACSDiva software (BD Bioscience).

Murine experiments

Mice were 8-12-week old C57BL/6J male or females (BL6, Jackson Labs). All mice were maintained in specific pathogen-free conditions. All animal studies were performed using procedures approved by the UTHSA Animal Care and Use Program. For experimental BC metastasis, male mice were challenged intravenously with 5 x 10^5 MB49 mouse BC cells. Surgery was a ventral 3 cm midline incision through the skin and peritoneum, followed

immediately by 2-layer closure using 4-0 vicryl suture (Ethicon J214H) to close peritoneum and 7 mm clips to close skin (CellPoint Scientific 203-1000), performed within 15 minutes of tumor challenge. Surgical anesthesia included ketamine HCl (JHP pharmaceuticals) at 80 mg/kg, xylazine (LLOYD) at 8 mg/kg, and acepromazine maleate (Boehringer Ingelheim Vetmedica) at 1 mg/kg in sterile PBS at a final volume of 300 μL/mouse/20 g body weight. On day 14 post tumor challenge, mice were euthanized, and lungs were harvested in 10% buffered formalin for subsequent H&E staining, and splenocytes were processed for flow cytometry staining using Fixable Viability Dye (eBioscience, Invitrogen), fluorochrome-conjugated monoclonal anti-mouse CD45 (clone 30-F11), CD3 (clone 17A2), PD-1 (clone 29F.1A12), Tim-3 (clone RMT3-23), and Lag-3 (clone C9B7W) (Biolegend). For orthotopic BC experiments, female mice were challenged with 80,000 MB49 cells as described (31) and treated with monoclonal anti-mouse PD-L1 (clone 10F.9G2, BioXcell) at 100 μg per mouse in 100 μL by intraperitoneal injection or equivalent isotype control rat IgG2b monoclonal antibody (clone LTF-2, BioXcell) on days 7, 12, 17. Mice were euthanized on day 21 for examination of retroperitoneal tumor-draining lymph nodes (TDLNs) by cytokine ELISPOT assay or followed for survival as noted.

ELISPOT assay

MultiScreen ImmunoSpot plates (Millipore) were coated with anti-mouse IFNγ capture monoclonal antibody (1 μg/mL; clone AN-18, BioLegend) at 4° C. overnight, followed by washes with sterile PBS, then blocked with 1% BSA (Sigma Aldrich) in sterile PBS at room temperature for 1 hour. 2.5 $x10^5$ TDLN cells in 100 μL complete RPMI (cR-10) medium containing 10% fetal bovine serum (HyClone, GE), 2 mM L-glutamine (Corning, Fisher), 100 IU penicillin, and streptomycin (100 μg/mL; Corning, Fisher) were added into each well. Another 100 μL of cR-10 was added to each well alone (medium control) or, plus 2.5 $x10^5$ irradiated (25Gy, γ-irradiator) MB49 cells. TDLN cells and tumor target cells were mixed and incubated at 37°C in a 5% CO_2 atmosphere for 24 hours. Wells were then washed and incubated with biotin-conjugated anti-mouse IFNγ detection monoclonal antibody (0.25 μg/mL; clone R4-6A2, BioLegend) at 4° C overnight. Wells were then incubated with 1:2000 streptavidin-AP (KPL) at room temperature for 1.5 hours, followed by washes and developed with BCIP/NBT phosphatase substrate (KPL). The reaction was stopped by deionized water after spots were formed. IFNγ-producing spot-forming cells (SFCs) were quantified using an ImmunoSpot analyzer (S6 Micro, CellularTechnology) with ImmunoSpot software, version 6.0 (Cellular Technology). Absolute SFC numbers in response to irradiated MB49 tumor cells were normalized by SFC in medium control for every TDLN sample.

Statistics

The primary trial objective was to test the PD response of rapamycin defined by a significant inhibition of S6 kinase 1 (S6K1) phosphorylation (comparing post-treatment to baseline values in tissue samples). Secondary trial objectives were to determine rapamycin bladder tissue concentrations and effects of rapamycin on circulating T lymphocytes. The trial sample size was based on the primary objective of identifying a pharmacodynamic (PD) treatment response in bladder tissue, defined as ≥60% inhibition in mTORC1 activity measured indirectly by phosphorylation of its downstream target ribosomal protein (rp) S6

on Ser 240/244 over total rpS6, based on a prior established benchmark (25). The change in mTORC1 activity was estimated using the change in the H-score for phospho (p)-rpS6/total rpS6 in the cystectomy tumor tissue compared with biopsy tumor tissue (25). The endpoint was mTORC1 inhibition (yes, no) in post treatment tissue. A sample size calculation was based on Fisher's exact test of H_o:p_T=p_C versus H_1:$p_T \neq p_C$ at α=0.05, where p_T and p_C are the proportions of treated and control patients experiencing a PD treatment response. Assuming p_C=0.10 and p_T=0.60, this study would attain 80% power for testing H_o with n=17 patients per group. An interim analysis was conducted following enrollment of the first 20 patients due to unexpected increase in rpS6 phosphorylation at time of cystectomy in control patients. Pathologic tumor downstaging was defined as clinical stage T2 and pathologic stage <T2 or clinical stage <T2 and pathologic stage ≤T2. Pathologic tumor upstaging was defined as clinical stage <T2 and pathologic stage ≥T2 or clinical stage T2 with pathologic stage >T2. A Pearson product-moment correlation coefficient was computed to assess the relationship between the blood and tissue rapamycin concentrations. A Spearman rank-order correlation coefficient was computed to assess the relationship between rapamycin concentrations and PD response due to violation of normality. Non-parametric data were represented as median [interquartile range (IQR)] and parametric data as mean [standard deviation (SD)]. Groups were contrasted on the median or mean with Wilcoxon or *t*-tests as appropriate and on binary outcomes with Fisher's exact test. The significance of within-patient changes on paired measurements taken before and after cystectomy was assessed by Wilcoxon signed rank test. To compare effects of anti-PD-L1 therapy on number of tumor-specific cells, we analyzed the significance of the difference in log-transformed median fold change between surgery and no surgery with two-sided testing on the group (surgery, no surgery) by a condition (IgG control, αPD-L1) interaction term in a linear model of log number of tumor-specific IFNγ spots. All statistical testing was two-sided with a significance level of 5% using PASS (version 11, Kaysville UT 2011) or Stata (version 10.1, College Station TX 2010).

Results

Study population and adverse events

20 patients were randomized, including 11 to rapamycin and 9 to control (patient and surgical characteristics detailed in Table 1). The adverse event (AE) rate was similar between groups: grade 3-4 AEs were observed in 7 of 11 (64%) patients receiving rapamycin and 6 of 9 (67%) control patients (Supplementary Table S1). Patients treated with rapamycin had a non-significant increase in complications related to healing (*i.e.*, fascia dehiscence, skin separation, or urinary anastomotic leak) compared to control patients (36% vs. 0%, respectively; P=0.09). Rapamycin concentrations were non-significantly higher among patients experiencing wound separation compared to patients without wound separation (9.74 ng/mL versus 6.50 ng/mL, P=0.27). Mean (standard deviation) time from biopsy to cystectomy was 34 days (15 days) for control patients and 44 days (9 days) for rapamycin-treated patients (P=0.06). Pathologic downstaging occurred in no patients treated with rapamycin and 2 (10%) of the control patients (P=0.19).

Rapamycin accumulates in bladder tissue and inhibits tumor mTORC1

mTORC1 responds to environmental nutrients to enhance protein synthesis by ribosome biogenesis via S6 kinase 1 (S6K1) phosphorylation of rpS6 (32). Thus, inhibition of rpS6 phosphorylation provides a useful read-out of rapamycin PD efficacy. Although the specified PD endpoint did not reach statistical significance (P=0.09), the study was concluded at the interim analysis because a significant difference between the median change in mTORC1 status between rapamycin-treated and control patients (P=0.008) was observed. The median p-/total rpS6 change (biopsy to cystectomy) was a 64% (IQR = 45% to 185%) increase in control patients and a 14% (IQR = −77% to 0%) decrease in rapamycin-treated patients with adequate paired tissue for evaluation (Fig. 1A–B), indicating a significant rapamycin PD effect in bladder tissue. No detectable difference in 4E-BP1 (another mTORC1 target rarely altered significantly by rapamycin) or phosphorylated AKT (a measure of mTORC2 activity) across treatment groups was seen (Supplementary Fig. S3).

The mean blood and bladder rapamycin concentrations in the remaining ten patients were 9.1 ng/mL (range, 3.5-13.3 ng/mL) and 17.2 (range, 7.8-42.2 ng/g). The slope of a best-fit line of rapamycin in tumors versus blood was 2.23, consistent with a 2-fold increase in rapamycin tissue concentrations over whole blood concentrations (r=0.67, P=0.03, Fig. 2A). Correlations were observed between PD effect of rapamycin and whole blood (r=−0.77, P=0.01) and tissue (r=−0.82, P=0.01) rapamycin concentrations (Fig. 2B). A rapamycin PD effect was observed in some patients, even at relatively low blood concentrations (<10 ng/mL), suggesting that rapamycin or rapamycin analogues could inhibit tumor rpS6 at much lower doses than currently used in cancer patients. Together, these findings confirm substantial rapamycin tissue penetration and tumor cell mTORC1 inhibition in BC using 3 mg orally/day.

Rapamycin does not suppress circulating T cells

mTOR inhibition enhances memory $CD8^+$ T-cell proliferation *in vitro* (33), improves antigen recall responses in mice (33,34), and boosts vaccine responses in humans (22). Therefore, modulation of T cells by mTOR inhibition could be therapeutic in cancer, but such immune effects in cancer patients are little studied (35–37). To address potential concerns for T-cell suppression, we evaluated T-cell changes during rapamycin therapy. Rapamycin increased $CD4^+$ and decreased $CD8^+$ circulating T-cell populations compared to control patients, but these effects were not statistically significant (Supplementary Fig. S4) and did not induce general T-cell lymphocytopenia (Supplementary Fig. S5). Similarly, no significant effects on memory or effector T cells, including $CD62L^+$ $CD45RO^+$ central memory $CD4^+$ or $CD8^+$ T cells (Supplementary Fig. S4) nor $CD4^+FoxP3^+$ regulatory T cells (Supplementary Fig. S4) was observed. Rapamycin had no significant effects on prevalence of $CD4^+$ or $CD8^+$ T cells producing IFNγ or TNFα antitumor cytokines (Supplementary Fig. S4). These findings indicate that at a dose of 3 mg daily for four weeks, rapamycin has no apparent immunosuppressive effects on circulating T cells.

Surgery induces T-cell exhaustion in human BC

Although surgery remains the mainstay for treating most solid cancers, surgical trauma promotes tumor progression. Proposed mechanisms include increased tumor cell

dissemination by mechanical manipulation, release of pro-angiogenic factors, and inhibition of cell-mediated immunity (38–40). Surgical trauma is associated with immunosuppression, including increased PD-1 expression on $CD4^+$ and $CD8^+$ T cells in the post-operative period consistent with T-cell exhaustion (39,41). We saw an increase in the proportion of circulating T cells expressing markers of exhaustion (PD-1, Tim-3, and Lag-3) following surgery (Fig. 3A), suggesting that cystectomy could induce surgery-mediated immune dysfunction. We examined function of circulating T cells from our patients by electronically sorting T cells into $PD\text{-}1^+$ and $PD\text{-}1^-$ populations. $PD\text{-}1^+$ T cells proliferated less than $PD\text{-}1^-$ T cells *in vitro* (Fig. 3B), consistent with functional exhaustion of $PD\text{-}1^+$ T cells. However, we found no significant difference in IFNγ or TNFα cytokine production between $PD\text{-}1^+$ and $PD\text{-}1^-$ T cells (Fig. 3C, Supplementary Fig. S2). The percentage of $CD4^+$ and $CD8^+$ T cells expressing PD-1 increased by more than 25-50% following surgery in our patients (Fig. 3D).

Patients treated with rapamycin had significantly fewer circulating $PD\text{-}1^+$ $CD4^+$ and $CD8^+$ T cells following surgery, suggesting that rapamycin could reduce surgery-mediated T-cell exhaustion (Fig. 3D). Examination of intratumoral lymphocytes revealed that patients treated with rapamycin had fewer tumor-infiltrating $PD\text{-}1^+CD8^+$ T cells on cystectomy tissue compared to matched biopsy specimens (P=0.047), whereas the control patients had similar proportions of $PD\text{-}1^+CD8^+$ T cells between biopsy and cystectomy specimens (P=0.1). Nevertheless, the percentage change between matched specimens was not statistically significant between rapamycin-treated and control patients (Supplementary Fig. S6A). Rapamycin had no discernable effect on intratumoral $PD\text{-}1^+CD4^+$ T cell populations (Supplementary Fig. S6A), and no effect on the percentage of PD-L1–expressing intratumoral lymphocytes. Rapamycin-treated patients had a significant increase in the proportion of PD-L1–expressing bladder tumor cells at cystectomy compared to matched biopsy specimens (P=0.04), whereas PD-L1 expression on bladder tumors from control patients did not change (P=0.79). However, the difference in the proportional change between rapamycin and control patients was not statistically significant (Supplementary Fig. S6B).

Surgery increases metastases and reduces anti–PD-L1 efficacy

To determine the potential impact of surgery-induced immune dysfunction in BC further, we studied the influence of surgery (midline 3 cm laparotomy) in mice challenged with syngeneic MB49 bladder tumors. In this model, surgery resulted in an increase in pulmonary metastasis and reduced survival associated with an increase in percentage of T cells expressing the exhaustion markers PD-1, TIM-3, and LAG-3 (Fig. 4A–B), providing further evidence of surgery-induced T-cell exhaustion. Surgery decreased the efficacy of anti–PD-L1 immunotherapy against orthotopic MB49 bladder tumors (Fig. 4C). Tumor-specific T cells that proliferate and release antitumor cytokines in response to tumor-specific antigens are essential for effective tumor control. As predicted, anti–PD-L1 immunotherapy increased the generation of tumor-specific cells in TDLNs, but surgery significantly reduced this effect (Fig. 4D). These findings indicate that surgery dampens tumor-specific immunity and clinical response during anti–PD-L1 BC immunotherapy.

Discussion

Tumor eradication by immune cells depends on effective T-cell mediated responses against tumor-specific antigens. Engagement of antigen by the T-cell receptor can lead to activation or anergy, depending on the context and degree of co-stimulation (42). mTOR integrates environmental signals, growth factors, and cytokines during antigen encounter to determine the fate of the T cell following T-cell receptor/antigen encounters (43) and, thus, can influence the activation versus anergy outcome. Initially rapamycin was thought to promote T-cell anergy by blocking cell cycle progression (44,45), but evidence shows that rapamycin can promote T-cell activation, increase memory effector T cells (19,46), and boost tumor antigen-specific memory responses during cancer therapy (19).

Studies in animal models show that surgery induces tumor progression (reviewed in (47)). Diverse mechanisms for surgery-induced tumor progression are proposed, including mechanical dissemination of tumor cells, trauma-induced release of vasculature growth factors, and specific dysfunction of natural killer and T cells (39,41). Because surgery did not induce T lymphocytopenia in our patients, post-cystectomy immunosuppression was likely due to reduced T-cell function as opposed to T-cell numbers, but further work is warranted in this area. We observed after surgery a substantial increase in PD-1^+ T cells that have exhaustion features in both humans and mice, and these changes were present 30 days after surgery, a time when adjuvant therapy is often initiated. Our pre-clinical BC model data suggests that surgery could abrogate efficacy of post-operative immune therapy, demonstrated by decreased efficacy of anti–PD-L1 therapy when given following a laparotomy without any organ removal. Therefore, surgery-induced immune dysfunction could influence response to immune therapy following surgery, and the timing of initiation of adjuvant therapy could be an important factor driving response to adjuvant therapy. Similar immunosuppressive effects are reported for patients undergoing surgery for lung cancer (39). Pulmonary lobectomy resulted in an increased prevalence of circulating dysfunctional PD-1^+ T cells in the early post-surgical period (39). We speculate that surgery leads to T-cell exhaustion, which contributes to the failure to eradicate minimal residual disease and the high relapse rates following cystectomy.

Findings here suggest a role for rapamycin in reducing surgery-induced T-cell dysfunction, which could lead to improved post-surgical outcomes. In patients undergoing cystectomy, rapamycin significantly reduced the prevalence of PD-1^+ $CD4^+$ and $CD8^+$ T cells, suggesting that rapamycin could reverse T-cell exhaustion. Rapamycin also decreased the percentage of intratumoral PD-1^+CD8^+ T cells. Although this effect was not significantly different than control patients, limited statistical power could be the cause, as sufficient matched-tissue was only available for 10 patients. Also, our evidence indicated that rapamycin could increase tumor PD-L1 expression, warranting further examination of rapamycin's effects on human tumor and tumor-infiltrating lymphocyte PD-1/PD-L1. Further, presurgical rapamycin could facilitate response to adjuvant immune therapy, which is currently under investigation.

When this study protocol was initiated, a dose of 3 mg daily rapamycin was chosen based on safety data in surgically treated cancer patients(25). However, preclinical data indicates that

lower doses could be even more effective at enhancing T-cell functions. At a dose of 75 μg/kg in mice (equivalent to ~0.5 mg daily in an 80 kg human), rapamycin enhances the survival of antigen-specific $CD8^+$ T cells and improves their functional qualities including antitumor effects (19,33). We previously showed that 75 μg/kg rapamycin improved T-cell activation, promoted T-cell memory, and augmented immunotherapy in a mouse melanoma model (18). Rapamycin-treated T cells exhibit long-term memory maintenance during homeostatic proliferation, allowing for recall responses upon exposure to antigen (33). Thus, distinct immune effects of low dose rapamycin could support antitumor effects and warrants further investigation.

Cystectomy is associated with a high perioperative complication rate (48,49) due, in part, to the patient population as BC is associated with advanced age and tobacco use. The perioperative complication rates among patients in this study were considerable, with more than half of patients experiencing a grade 3-4 AE, and many patients experienced more than one serious complication. A concerning higher rate of wound complications in the rapamycin-treated group was seen, and despite meticulous closure with absorbable sutures, it is possible that the continuation of rapamycin up until the day of surgery contributed to poor wound healing. This is particularly relevant during cystectomy operations, due to comorbidities of patients, the length of surgery, and the need for bowel reconstruction. These findings support discontinuation of any dose mTOR inhibition at least 5-10 days before planned surgery and consideration of interrupted fascial suture closure for complex wounds (26). Future work assessing lower rapamycin doses that ours (18) and other's (19) animal data predict will still provide meaningful immune improvement.

There are limitations to this study. We did not account for tumor heterogeneity, as immunohistochemistry staining results were summarized after examining all stained tumor tissue without comparing specific subsections of tumors between biopsy and cystectomy specimens. Thus, the apparent increase in rpS6 phosphorylation in control subjects' biopsy versus cystectomy specimens could reflect issues related to variations of rpS6 phosphorylation in distinct areas (*e.g.*, peripheral versus central location) of bladder tumors, for which we were unable to address but is a topic that requires further investigation. Time from biopsy to cystectomy was longer for patients treated with rapamycin compared to control, and therefore, differences between groups could be influenced by lack of identical times for blood collection. Additional time points during rapamycin treatment were not assessed but could be informative. Finally, although we are interested in immune effects of rapamycin, there was insufficient material from these patients to evaluate rapamycin PD effects on T-cell mTOR signals. We have previously shown that even low rapamycin doses can suppress T-cell mTOR(18,50) and, thus, additional work is needed.

In conclusion, our data examined effects of low dose rapamycin on tumor mTOR, T-cell exhaustion, and tolerability in patients undergoing major surgery for BC. Surgery induced significant immune effects, suggested from our human data, and supported by our pre-clinical mouse BC model that was associated with decreased efficacy of post-operative cancer immune therapy. Altogether, existing data and our present data suggest that lower dose rapamycin could be an effective treatment for BC through direct effects on tumor and/or indirectly through modulating T-cell function.

Supplementary Material

Refer to Web version on PubMed Central for supplementary material.

Acknowledgments

Funding: (1) 8KL2 TR000118, K23, (2) the Mays Family Cancer Center at University of Texas Health San Antonio (P30 CA054174), (3) the Roger L. And Laura D. Zeller Charitable Foundation Chair in Urologic Cancer, (4) the Max & Minnie Tomerlin Voelcker Fund, (5) the Skinner endowment, (6) the Barker Foundation, (7) the Owens Foundation and (8) The Clayton Foundation

References

1. Platt FM, Hurst CD, Taylor CF, Gregory WM, Harnden P, Knowles MA. Spectrum of phosphatidylinositol 3-kinase pathway gene alterations in bladder cancer. Clin Cancer Res 2009;15(19):6008–17 doi 10.1158/1078-0432.CCR-09-0898. [PubMed: 19789314]
2. Meeks JJ, Lerner SP. Molecular Landscape of Non-Muscle Invasive Bladder Cancer. Cancer Cell 2017;32(5):550–1 doi 10.1016/j.ccell.2017.08.015. [PubMed: 29136502]
3. Liu ST, Hui G, Mathis C, Chamie K, Pantuck AJ, Drakaki A. The Current Status and Future Role of the Phosphoinositide 3 Kinase/AKT Signaling Pathway in Urothelial Cancer: An Old Pathway in the New Immunotherapy Era. Clin Genitourin Cancer 2018;16(2):e269–e76 doi 10.1016/j.clgc.2017.10.011. [PubMed: 29199023]
4. Nickerson ML, Witte N, Im KM, Turan S, Owens C, Misner K, et al. Molecular analysis of urothelial cancer cell lines for modeling tumor biology and drug response. Oncogene 2017;36(1):35–46 doi 10.1038/onc.2016.172. [PubMed: 27270441]
5. Bagrodia A, Krabbe LM, Gayed BA, Kapur P, Bernstein I, Xie XJ, et al. Evaluation of the prognostic significance of altered mammalian target of rapamycin pathway biomarkers in upper tract urothelial carcinoma. Urology 2014;84(5):1134–40 doi 10.1016/j.urology.2014.07.050. [PubMed: 25443916]
6. Winters BR, Vakar-Lopez F, Brown L, Montgomery B, Seiler R, Black PC, et al. Mechanistic target of rapamycin (MTOR) protein expression in the tumor and its microenvironment correlates with more aggressive pathology at cystectomy. Urol Oncol 2018;36(7):342 e7–e14 doi 10.1016/j.urolonc.2018.03.016.
7. Madka V, Mohammed A, Li Q, Zhang Y, Biddick L, Patlolla JM, et al. Targeting mTOR and p53 Signaling Inhibits Muscle Invasive Bladder Cancer In Vivo. Cancer Prev Res (Phila) 2016;9(1):53–62 doi 10.1158/1940-6207.CAPR-15-0199. [PubMed: 26577454]
8. Makhlin I, Zhang J, Long CJ, Devarajan K, Zhou Y, Klein-Szanto AJ, et al. The mTOR pathway affects proliferation and chemosensitivity of urothelial carcinoma cells and is upregulated in a subset of human bladder cancers. BJU Int 2011;108(2 Pt 2):E84–90 doi 10.1111/j.1464-410X.2010.09844.x. [PubMed: 21050361]
9. Seager CM, Puzio-Kuter AM, Patel T, Jain S, Cordon-Cardo C, Mc Kiernan J, et al. Intravesical delivery of rapamycin suppresses tumorigenesis in a mouse model of progressive bladder cancer. Cancer Prev Res (Phila) 2009;2(12):1008–14 doi 10.1158/1940-6207.CAPR-09-0169. [PubMed: 19952358]
10. Fechner G, Classen K, Schmidt D, Hauser S, Muller SC. Rapamycin inhibits in vitro growth and release of angiogenetic factors in human bladder cancer. Urology 2009;73(3):665–8; discussion 8-9 doi 10.1016/j.urology.2008.09.070. [PubMed: 19081609]
11. Bachir BG, Souhami L, Mansure JJ, Cury F, Vanhuyse M, Brimo F, et al. Phase I Clinical Trial of Everolimus Combined with Trimodality Therapy in Patients with Muscle-Invasive Bladder Cancer. Bladder Cancer 2017;3(2):105–12 doi 10.3233/BLC-160090. [PubMed: 28516155]
12. Pinto-Leite R, Arantes-Rodrigues R, Ferreira R, Palmeira C, Colaco A, Moreira da Silva V, et al. Temsirolimus improves cytotoxic efficacy of cisplatin and gemcitabine against urinary bladder cancer cell lines. Urol Oncol 2014;32(1):41 e11–22 doi 10.1016/j.urolonc.2013.04.012.

13. Vasconcelos-Nobrega C, Pinto-Leite R, Arantes-Rodrigues R, Ferreira R, Brochado P, Cardoso ML, et al. In vivo and in vitro effects of RAD001 on bladder cancer. Urol Oncol 2013;31(7):1212–21 doi 10.1016/j.urolonc.2011.11.002. [PubMed: 22169072]

14. Chiong E, Lee IL, Dadbin A, Sabichi AL, Harris L, Urbauer D, et al. Effects of mTOR inhibitor everolimus (RAD001) on bladder cancer cells. Clin Cancer Res 2011;17(9):2863–73 doi 10.1158/1078-0432.ccr-09-3202. [PubMed: 21415218]

15. Gerullis H, Eimer C, Ecke TH, Georgas E, Freitas C, Kastenholz S, et al. A phase II trial of temsirolimus in second-line metastatic urothelial cancer. Med Oncol 2012;29(4):2870–6 doi 10.1007/s12032-012-0216-x. [PubMed: 22447503]

16. Milowsky MI, Iyer G, Regazzi AM, Al-Ahmadie H, Gerst SR, Ostrovnaya I, et al. Phase II study of everolimus in metastatic urothelial cancer. BJU Int 2013;112(4):462–70 doi 10.1111/j.1464-410X.2012.11720.x. [PubMed: 23551593]

17. Seront E, Rottey S, Sautois B, Kerger J, D'Hondt LA, Verschaeve V, et al. Phase II study of everolimus in patients with locally advanced or metastatic transitional cell carcinoma of the urothelial tract: clinical activity, molecular response, and biomarkers. Ann Oncol 2012;23(10):2663–70 doi 10.1093/annonc/mds057. [PubMed: 22473592]

18. Liu Y, Pandeswara S, Dao V, Padron A, Drerup JM, Lao S, et al. Biphasic rapamycin effects in lymphoma and carcinoma treatment. Cancer Res 2016 doi 10.1158/0008-5472.CAN-16-1140.

19. Pedicord VA, Cross JR, Montalvo-Ortiz W, Miller ML, Allison JP. Friends not foes: CTLA-4 blockade and mTOR inhibition cooperate during CD8+ T cell priming to promote memory formation and metabolic readiness. J Immunol 2015;194(5):2089–98 doi 10.4049/jimmunol.1402390. [PubMed: 25624453]

20. Hurez V, Dao V, Liu A, Pandeswara S, Gelfond J, Sun L, et al. Chronic mTOR inhibition in mice with rapamycin alters T, B, myeloid, and innate lymphoid cells and gut flora and prolongs life of immune-deficient mice. Aging Cell 2015 doi 10.1111/acel.12380.

21. Guri Y, Nordmann TM, Roszik J. mTOR at the Transmitting and Receiving Ends in Tumor Immunity. Frontiers in immunology 2018;9:578 doi 10.3389/fimmu.2018.00578. [PubMed: 29662490]

22. Mannick JB, Del Giudice G, Lattanzi M, Valiante NM, Praestgaard J, Huang B, et al. mTOR inhibition improves immune function in the elderly. Sci Transl Med 2014;6(268):268ra179 doi 10.1126/scitranslmed.3009892.

23. Barber DL, Wherry EJ, Masopust D, Zhu B, Allison JP, Sharpe AH, et al. Restoring function in exhausted CD8 T cells during chronic viral infection. Nature 2006;439(7077):682–7 doi 10.1038/nature04444. [PubMed: 16382236]

24. Ahmadzadeh M, Johnson LA, Heemskerk B, Wunderlich JR, Dudley ME, White DE, et al. Tumor antigen-specific CD8 T cells infiltrating the tumor express high levels of PD-1 and are functionally impaired. Blood 2009;114(8):1537–44 doi 10.1182/blood-2008-12-195792. [PubMed: 19423728]

25. Armstrong AJ, Netto GJ, Rudek MA, Halabi S, Wood DP, Creel PA, et al. A pharmacodynamic study of rapamycin in men with intermediate- to high-risk localized prostate cancer. Clin Cancer Res 2010;16(11):3057–66 doi 10.1158/1078-0432.CCR-10-0124. [PubMed: 20501622]

26. Campistol JM, Cockwell P, Diekmann F, Donati D, Guirado L, Herlenius G, et al. Practical recommendations for the early use of m-TOR inhibitors (sirolimus) in renal transplantation. Transpl Int 2009;22(7):681–7 doi 10.1111/j.1432-2277.2009.00858.x. [PubMed: 19386082]

27. Hasty P, Livi CB, Dodds SG, Jones D, Strong R, Javors M, et al. eRapa restores a normal life span in a FAP mouse model. Cancer Prev Res (Phila) 2014;7(1):169–78 doi 10.1158/1940-6207.CAPR-13-0299. [PubMed: 24282255]

28. Livi CB, Hardman RL, Christy BA, Dodds SG, Jones D, Williams C, et al. Rapamycin extends life span of Rb1+/− mice by inhibiting neuroendocrine tumors. Aging (Albany NY) 2013;5(2):100–10 doi 10.18632/aging.100533. [PubMed: 23454836]

29. Harrison DE, Strong R, Sharp ZD, Nelson JF, Astle CM, Flurkey K, et al. Rapamycin fed late in life extends lifespan in genetically heterogeneous mice. Nature 2009;460(7253):392–5 doi nature08221 [pii] 10.1038/nature08221. [PubMed: 19587680]

30. Ishibashi H, Suzuki T, Suzuki S, Moriya T, Kaneko C, Takizawa T, et al. Sex steroid hormone receptors in human thymoma. The Journal of clinical endocrinology and metabolism 2003;88(5): 2309–17 doi 10.1210/jc.2002-021353. [PubMed: 12727990]

31. Svatek RS, Zhao XR, Morales EE, Jha MK, Tseng TY, Hugen CM, et al. Sequential Intravesical Mitomycin plus Bacillus Calmette-Guerin for Non-Muscle-Invasive Urothelial Bladder Carcinoma: Translational and Phase I Clinical Trial. Clin Cancer Res 2015;21(2):303–11 doi 10.1158/1078-0432.CCR-14-1781. [PubMed: 25424854]

32. Chauvin C, Koka V, Nouschi A, Mieulet V, Hoareau-Aveilla C, Dreazen A, et al. Ribosomal protein S6 kinase activity controls the ribosome biogenesis transcriptional program. Oncogene 2014;33(4):474–83 doi 10.1038/onc.2012.606. [PubMed: 23318442]

33. Araki K, Turner AP, Shaffer VO, Gangappa S, Keller SA, Bachmann MF, et al. mTOR regulates memory CD8 T-cell differentiation. Nature 2009;460(7251):108–12 doi 10.1038/nature08155. [PubMed: 19543266]

34. Jagannath C, Lindsey DR, Dhandayuthapani S, Xu Y, Hunter RL Jr., Eissa NT. Autophagy enhances the efficacy of BCG vaccine by increasing peptide presentation in mouse dendritic cells. Nat Med 2009;15(3):267–76 doi 10.1038/nm.1928. [PubMed: 19252503]

35. Beziaud L, Mansi L, Ravel P, Marie-Joseph EL, Laheurte C, Rangan L, et al. Rapalogs Efficacy Relies on the Modulation of Antitumor T-cell Immunity. Cancer Res 2016;76(14):4100–12 doi 10.1158/0008-5472.CAN-15-2452. [PubMed: 27197194]

36. Kobayashi M, Kubo T, Komatsu K, Fujisaki A, Terauchi F, Natsui S, et al. Changes in peripheral blood immune cells: their prognostic significance in metastatic renal cell carcinoma patients treated with molecular targeted therapy. Med Oncol 2013;30(2):556 doi 10.1007/s12032-013-0556-1. [PubMed: 23539200]

37. Santoni M, Berardi R, Amantini C, Burattini L, Santini D, Santoni G, et al. Role of natural and adaptive immunity in renal cell carcinoma response to VEGFR-TKIs and mTOR inhibitor. Int J Cancer 2014;134(12):2772–7 doi 10.1002/ijc.28503. [PubMed: 24114790]

38. Tai LH, Tanese de Souza C, Sahi S, Zhang J, Alkayyal AA, Ananth AA, et al. A mouse tumor model of surgical stress to explore the mechanisms of postoperative immunosuppression and evaluate novel perioperative immunotherapies. J Vis Exp 2014(85) doi 10.3791/51253.

39. Xu P, Zhang P, Sun Z, Wang Y, Chen J, Miao C. Surgical trauma induces postoperative T-cell dysfunction in lung cancer patients through the programmed death-1 pathway. Cancer Immunol Immunother 2015;64(11):1383–92 doi 10.1007/s00262-015-1740-2. [PubMed: 26183035]

40. Ananth AA, Tai LH, Lansdell C, Alkayyal AA, Baxter KE, Angka L, et al. Surgical Stress Abrogates Pre-Existing Protective T Cell Mediated Anti-Tumor Immunity Leading to Postoperative Cancer Recurrence. PLoS One 2016;11(5):e0155947 doi 10.1371/journal.pone.0155947. [PubMed: 27196057]

41. Arai Y, Saito H, Ikeguchi M. Upregulation of TIM-3 and PD-1 on CD4+ and CD8+ T Cells Associated with Dysfunction of Cell-Mediated Immunity after Colorectal Cancer Operation. Yonago Acta Med 2012;55(1):1–9. [PubMed: 24031134]

42. Chen L, Flies DB. Molecular mechanisms of T cell co-stimulation and co-inhibition. Nat Rev Immunol 2013;13(4):227–42 doi 10.1038/nri3405. [PubMed: 23470321]

43. Delgoffe GM, Powell JD. mTOR: taking cues from the immune microenvironment. Immunology 2009;127(4):459–65 doi 10.1111/j.1365-2567.2009.03125.x. [PubMed: 19604300]

44. Powell JD, Lerner CG, Schwartz RH. Inhibition of cell cycle progression by rapamycin induces T cell clonal anergy even in the presence of costimulation. J Immunol 1999;162(5):2775–84. [PubMed: 10072524]

45. Vanasek TL, Khoruts A, Zell T, Mueller DL. Antagonistic roles for CTLA-4 and the mammalian target of rapamycin in the regulation of clonal anergy: enhanced cell cycle progression promotes recall antigen responsiveness. J Immunol 2001;167(10):5636–44. [PubMed: 11698435]

46. Zheng Y, Collins SL, Lutz MA, Allen AN, Kole TP, Zarek PE, et al. A role for mammalian target of rapamycin in regulating T cell activation versus anergy. J Immunol 2007;178(4):2163–70. [PubMed: 17277121]

47. Lejeune FJ. Is surgical trauma prometastatic? Anticancer Res 2012;32(3):947–51. [PubMed: 22399615]

48. Svatek RS, Fisher MB, Matin SF, Kamat AM, Grossman HB, Nogueras-Gonzalez GM, et al. Risk factor analysis in a contemporary cystectomy cohort using standardized reporting methodology and adverse event criteria. J Urol 2010;183(3):929–34 doi 10.1016/j.juro.2009.11.038. [PubMed: 20083264]

49. Shabsigh A, Korets R, Vora KC, Brook CM, Cronin AM, Savage C, et al. Defining Early Morbidity of Radical Cystectomy for Patients with Bladder Cancer Using a Standardized Reporting Methodology. Eur Urol 2008.

50. Dao V, Liu Y, Pandeswara S, Svatek RS, Gelfond JA, Liu A, et al. Immune-Stimulatory Effects of Rapamycin Are Mediated by Stimulation of Antitumor gammadelta T Cells. Cancer Res 2016;76(20):5970–82 doi 10.1158/0008-5472.CAN-16-0091. [PubMed: 27569211]

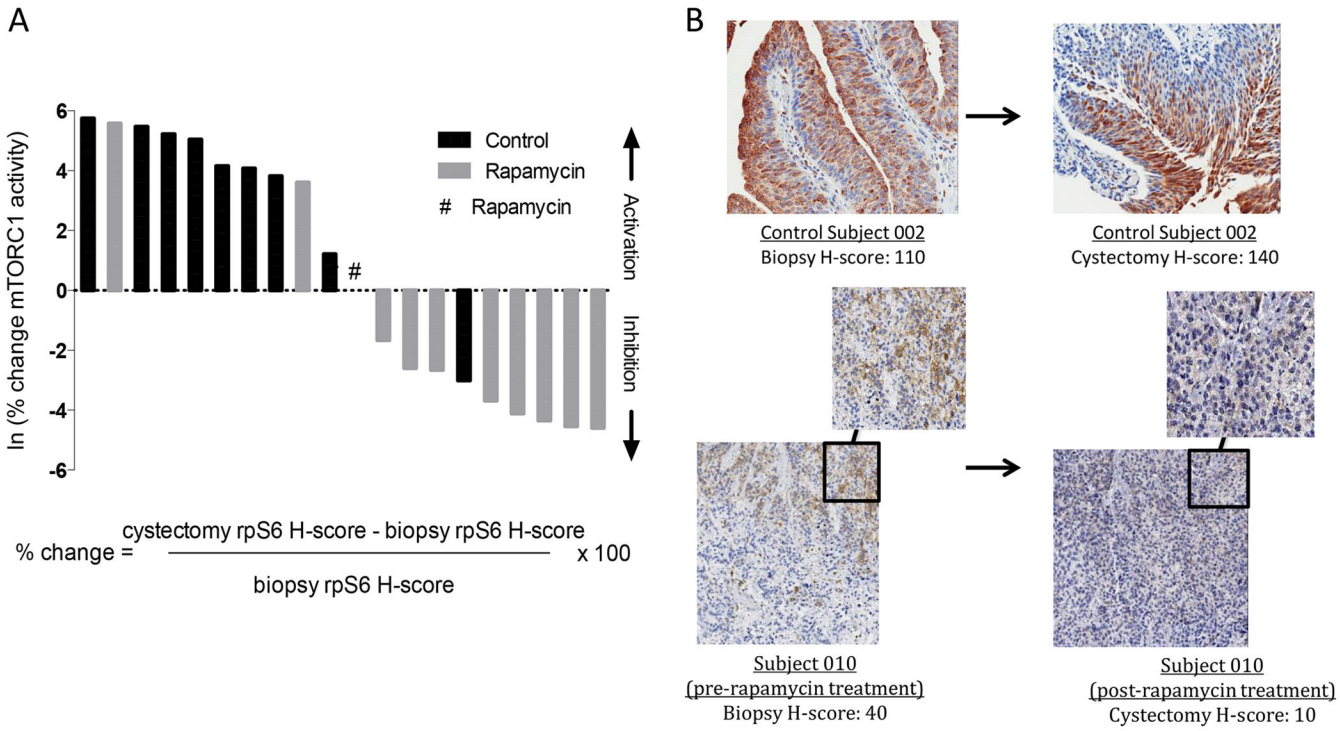

Figure 1. Rapamycin inhibits rpS6 kinase in BC.

Following biopsy of bladder tumors, patients with invasive BC were randomized to receive rapamycin (3 mg orally daily for 30 days) or no rapamycin prior to cystectomy. Blood and tissue concentrations of rapamycin were assessed on day 30, at time of cystectomy. For PD assessment, pre-treatment (biopsy) tissue was compared to post-treatment (cystectomy) tissue. (**A**) Waterfall bar plot showing primary PD end point, rpS6 kinase phosphorylation inhibition, in paired BC tissues [biopsy and cystectomy cancer tissue] among rapamycin-treated (n=11) and control (n=9) subjects. Percentage (%) change in phospho (p)/total (t) rpS6 (before and after rapamycin/ control) was calculated using the equation shown. (**B**) Representative IHC of staining for phosphorylated (Ser240/244) rpS6 of control subject 002 and rapamycin-treated subject 010 with H-score depicted. Data are from one representative experiment.

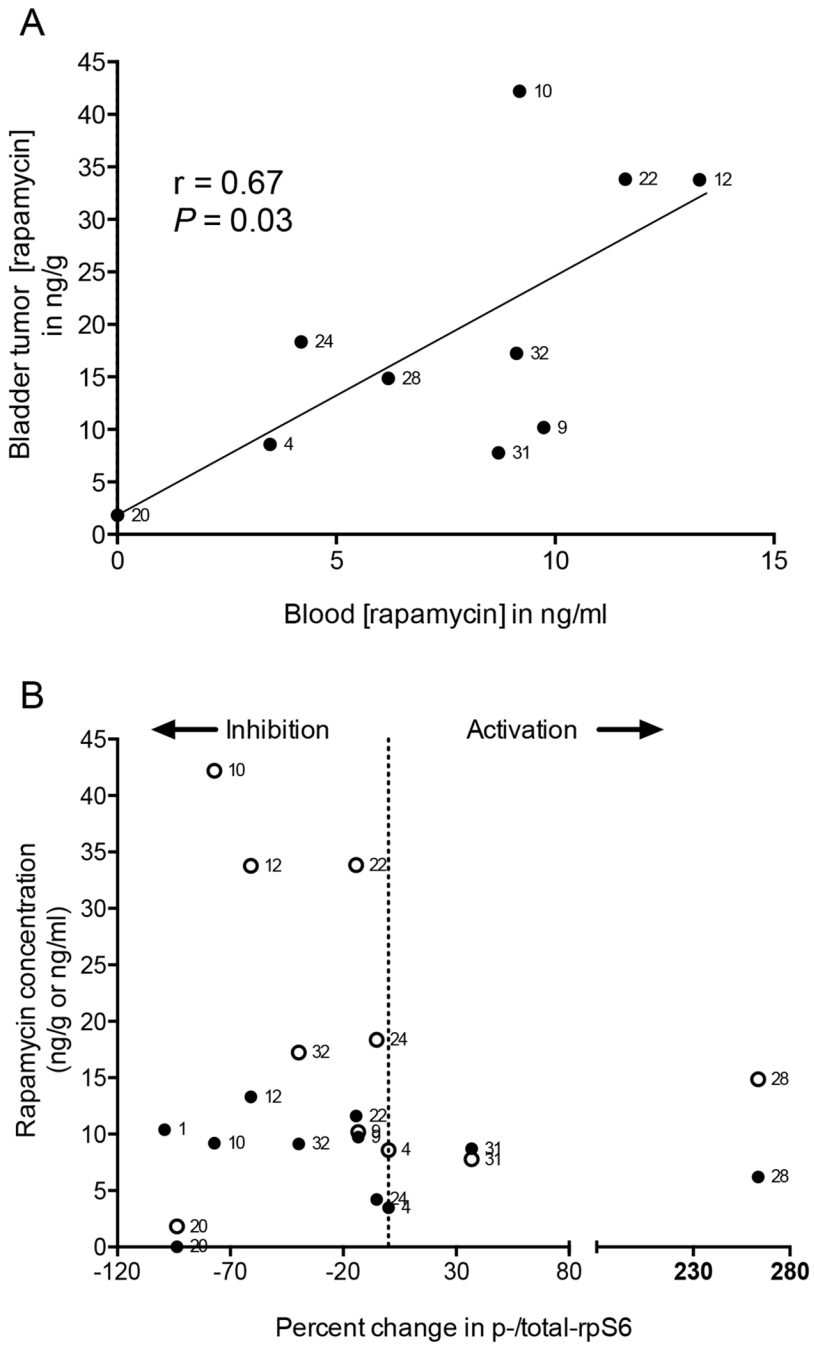

Figure 2. Rapamycin concentrations and PD effects in BC.

For patients on treatment, blood and tissue concentrations of rapamycin were analyzed 30 days after randomization (time of cystectomy) and measured using mass spectrometry. (**A**) Scatter plot showing individual blood and corresponding bladder tumor tissue rapamycin concentrations. Number next to each point represents subject number. *P* represents two-tailed test of Pearson correlation coefficient (r) for n=10 patients with available rapamycin concentrations. P value threshold for significance ≤0.05. (**B**) Scatter plot showing individual rapamycin bladder tumor tissue concentrations (filled symbols expressed as ng/g) and

peripheral blood concentrations (open symbols expressed as ng/mL) across percentage change in p-/total rpS6 (before and after rapamycin) among rapamycin-treated patients with evaluable tissue for biomarker assessment (n=11). Vertical line at 0% change in p-/total rpS6 defines activation versus inhibition. Data are from one representative experiment.

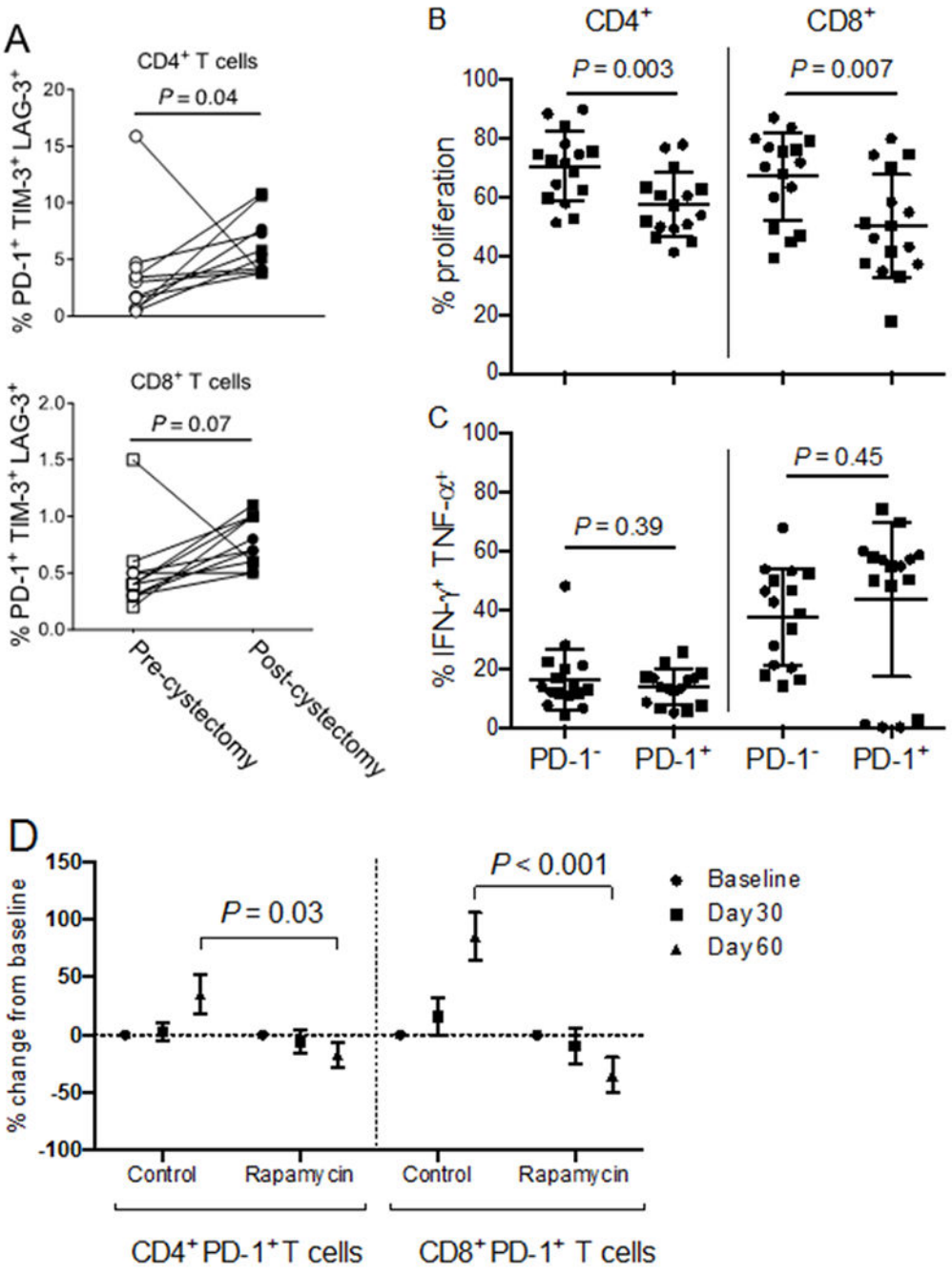

Figure 3. PD-1^{+} T cells are less proliferative than PD-1^{-} T cells in patients with BC, and rapamycin decreases T-cell exhaustion.

Peripheral blood mononuclear cells (PBMCs) from patients on trial. **(A)** Patients (n=11) with sufficient PBMCs were analyzed at baseline (before cystectomy) and at 60 days from registration. Phenotypes were determined using flow cytometry gated from live CD45^{+}CD3^{+}CD4^{+} (top) or CD45^{+}CD3^{+}CD8^{+} (bottom) lymphocytes. Proportion of cells co-expressing LAG-3, TIM-3, and PD-1 was analyzed. *P*: two-tailed Wilcoxin matched-pairs signed rank test. (**B**-**C**) PBMCs were sorted to high purity based on CD3^{+}PD-1^{+} versus

$CD3^+PD\text{-}1^-$ T cell surface expression using fluorescence-activated cell sorting (n=16 patients). Cells were stained with CFSE and stimulated *in vitro* with CD3/CD28 Dynabeads in a 1:1 cell to bead ratio. After three days, cells were stained for CD4 and CD8 and analyzed using flow cytometry for **(B)** proliferation or **(C)** cytokine expression. *P*: unpaired, two-tailed t tests. Circles represent control patients (n=8). Squares represent rapamycin-treated patients (n=8). **(D)** The proportion of $PD\text{-}1^+$ T cells among live $CD45^+CD3^+CD4^+$ and live $CD45^+CD3^+CD8^+$ T cells was determined using flow cytometry and analyzed as a percentage change from baseline for patient with sufficient material (n=8 controls and n=9 rapamycin). Results shown as mean±SEM. The mean values at specified time points were compared for control versus rapamycin-treated groups. *P*: unpaired, two-tailed *t*-tests. P value threshold for significance < 0.05. Data are from one representative experiment.

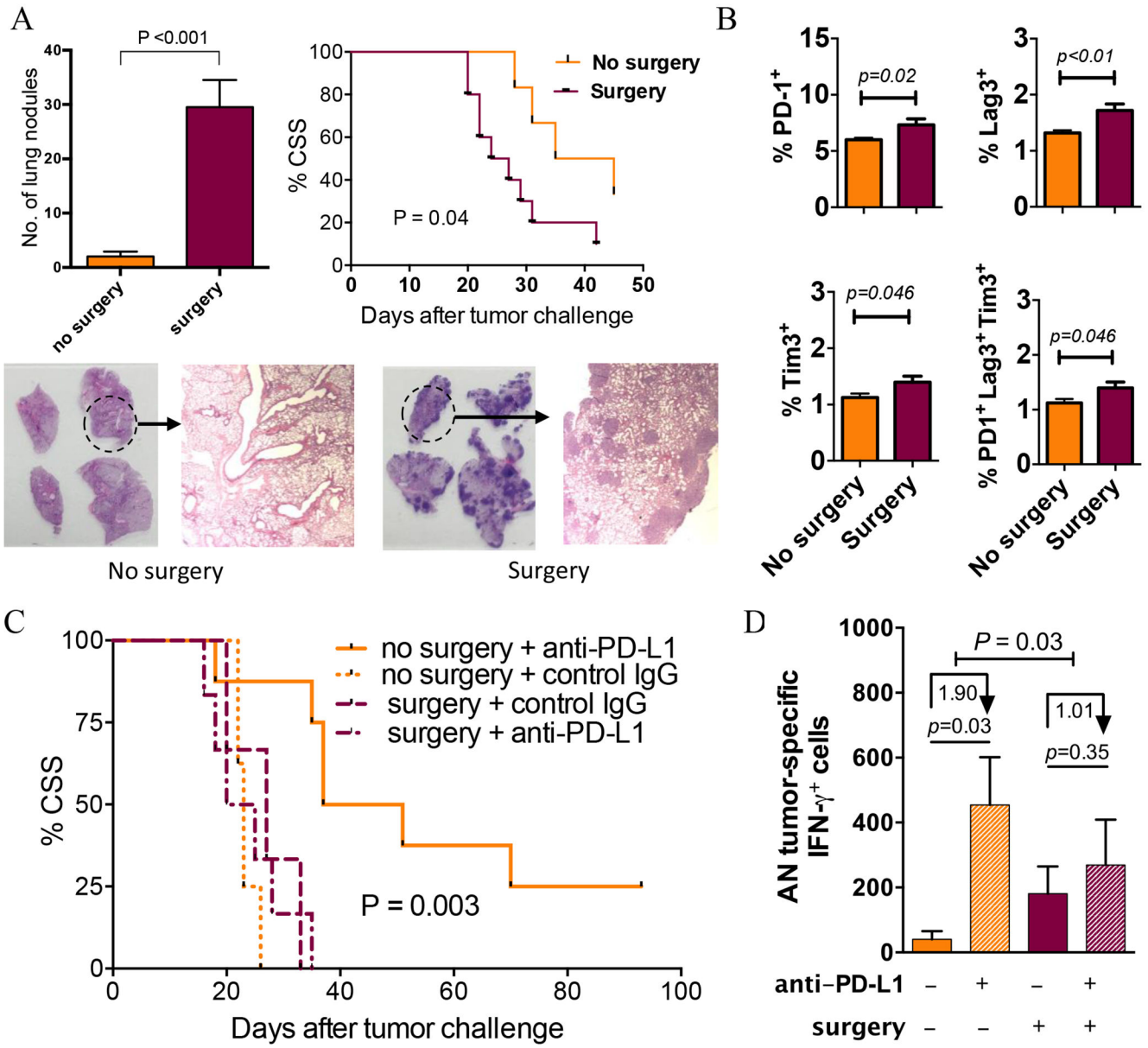

Figure 4. Surgery promotes BC growth and inhibits antitumor immunity in mice.

(**A-B**) C57Bl/6 (BL6) male mice (n=6/group) were challenged intravenously with MB49 tumor cells then anesthetized and subjected to 3 cm ventral laparotomy (surgery) versus no surgery. Mice were followed for cancer-specific survival (CSS, metastasis confirmed by necropsy) or sacrificed on day 14. (**A**) Lungs were analyzed for the presence of tumors (mean±SEM on y-axis), quantified by gross examination (representative samples of lung sections from one control and surgery mice shown), and confirmed with histopathology. CSS with and without surgery shown. (**B**) Cell surface exhaustion markers were detected and measured for splenic T cells. N=7-10 mice/group. *P*: two-tailed *t* test. (**C**) BL6 female mice were challenged orthotopically with MB49 tumor cells then subjected to surgery versus no surgery and given anti–PD-L1 or isotype control antibody on days 7, 12, and 17. N=6-8 mice/group. Survival compared between surgery + anti–PD-L1 versus no surgery + anti–PD-

L1 treated mice using log-rank test (significance shown as P). (**D**) In similar experiments with n=5 mice/group, bladder tumor-draining lymph nodes (TDLNs) were harvested on day 15 after tumor challenge. TDLN cells (0.25×10^6 cells per well) were recalled *ex vivo* by incubating with irradiated MB49 cells in 1:1 cell TDLN to MB49 cell ratio, and absolute number (AN) of tumor-specific IFNγ-producing cells per TDLN were quantified by ELISPOT assay. Numbers under arrows represent median log-fold change between groups. *P* indicates the significance of the difference in fold change between surgery and no surgery assessed with two-sided testing on the group (surgery, no surgery) by condition (IgG control, anti–PD-L1) interaction term in a linear model of the number of tumor-specific IFNγ in log units. All other p values represent two-tailed *t*-tests. Data are from a representative experiment that was repeated with similar results.

Table 1.

Baseline and pathologic characteristics of study participants

	Total	Rapamycin	Control
Median age (IQR)	70 (66-75)	67 (65-71)	74 (69-75)
Gender			
Female	3 (15%)	1 (9%)	2 (22%)
Male	17 (85%)	10 (91%)	7 (78%)
Race			
Hispanic	6 (30%)	2 (18%)	4 (44%)
Non-Hispanic	14 (70%)	9 (82%)	5 (56%)
Median weight (IQR)	80 kg (69-92)	80 kg (68-94)	79 kg (67-90)
Median BMI (IQR)	27 (24-30)	28 (24-29)	27 (23-32)
Clinical stage			
T1	6 (30%)	3 (27%)	2 (22%)
T2	11 (55%)	6 (55%)	6 (67%)
T3-T4	3 (15%)	2 (18%)	1 (11%)
Pathologic stage			
<T2	6 (30%)	3 (27%)	3 (33%)
T2	7 (35%)	3 (27%)	4 (44%)
T3	7 (35%)	5 (45%)	2 (22%)
Pathologic stage migration			
Down stage	2 (10%)	0 (0%)	2 (22%)
Same stage	12 (60%)	8 (73%)	4 (44%)
Upstaging	6 (30%)	4 (36%)	3 (33%)
Mean (SD) lymph nodes	30.8 (20.9)	30.3 (23.7)	31.3 (18.1)
Mean (SD) positive nodes	0.3 (0.6)	0.1 (0.3)	0.5 (.9)

BMI- body mass index, SD – standard deviation, IQR -interquartile range, kg-kilograms